Synthesis and Characterization of PEDOT Derivative with Carboxyl Group and Its Chemo Sensing Application as Enhanced Optical Materials

Dufen Hu, Long Zhang, Kaixin Zhang, Xuemin Duan, Jingkun Xu, Liqi Dong, Hui Sun, Xiaofei Zhu, Shijie Zhen

School of Pharmacy, Jiangxi Science and Technology Normal University, Nanchang 330013, People's Republic of China
Correspondence to: X. Duan (E-mail: duanxuemin@126.com) and J. Xu (E-mail: xujingkun@tsinghua.org.cn)

ABSTRACT: Poly(4-(((2,3-dihydrothieno[3,4-b][1,4]dioxin-2-yl)methoxy)methyl)benzoic acid) (PEDOT-Ph-COOH) was facilely synthesized by the direct electropolymerization of 4-(((2,3-dihydrothieno[3,4-b][1,4]dioxin-2-yl)methoxy)methyl)benzoic acid (EDOT-Ph-COOH) in CH_2Cl_2-Bu_4NPF_6 (0.10 M) system, and the PEDOT-Ph-COOH films were systematically investigated. The results displayed that the film had excellent reversible redox activities, good electrochemical performance, and rough and compact surface. Finally, the PEDOT-Ph-COOH film was used as an optical chemo-sensor for the highly selective and sensitive detection of F^-, PO_4^{3-}, HCO_3^-, $S_2O_3^{2-}$, Cu^{2+}, and Fe^{3+} in dimethyl sulfoxide. Satisfactory results indicated that optical chemo-sensor based on PEDOT-Ph-COOH possessed an excellent sensing performance and enhanced optical response, and it might be as potential promising materials, such as electrochromic devices, supercapacitors and so on. © 2014 Wiley Periodicals, Inc. J. Appl. Polym. Sci. **2015**, *132*, 41559.

INTRODUCTION

Among the numerous polymers that have been developed and studied over the past decades, poly(3,4-ethylenedioxythiophene) (PEDOT) is presented as one of the most promising conducting polymers of polythiophene (PTh) series from both a fundamental and practical perspective.[1] In comparison with other PTh derivatives, PEDOT possesses several inherently advantageous properties. It combines a low oxidation potential and moderate bandgap (1.6 vs. 2.2 eV) with a good stability in the oxidized state.[1–5] Also, PEDOT is found to be high conductivity (ca. 400–600 Scm^{-1}) for both chemically and electrochemically prepared samples.[6,7] In addition, PEDOT is almost transparent and highly stable in thin oxidized films.[1–8] A variety of potential applications have been explored in electrode materials, electronic materials, photoluminescent, membranes, electrochromic devices, supercapacitors, antistatic coatings, corrosion inhibitors, superhydrophobic fiber, energy storage, solar cells, and chemo/bio-sensor devices owing to these advantages.[9–23] According to recent reports, highly attention paid on potential practical applications of PEDOT is found to sharply increase, especially applications of PEDOT in chemo/bio-sensors area.[24]

Although the exploration of the field on PEDOT has become increasingly sophisticated, it still possesses some flaws: The optical absorption coefficient of PEDOT is relatively low (7.1 × 10^3 cm^{-1} at 2.1 eV) and the solubility of PEDOT in water needs be improved by addition of surfactant and introduction of pendant lyophilic groups, which limits its wide applications as optoelectronics and advanced composite materials.[25–27] Therefore, a series of new-generation PEDOT derivatives have been designed and synthesized to overcome these shortcomings and study potential improvements of PEDOT.[24,28–30] Solubility and optical activity can be enhanced by replacing the ethylene dioxide side group by adding alkoxy side chains or an alkyl group to the ethylenic carbon.[28] Subsequently, many research groups have explored and developed a variety of PEDOT derivatives by introducing different functional groups onto PEDOT to obtain new materials with excellent performance.[31–34] In recent years, Yu and co-workers[35,36] synthesized COOH-functionalized 3,4-ethylenedioxythiophene (EDOT) derivatives, and electropolymerized thin PEDOT films exhibited good biocompatibility, low intrinsic cytotoxicity, and displayed no inflammatory response upon implantation, making them ideal for biosensing and bioengineering applications.

Additional Supporting Information may be found in the online version of this article.

Inspired by these advantages, a novel strategy was designed for synthesis and electropolymerization of a carboxylic group functionalized EDOT derivative, poly(4-(((2,3-dihydrothieno[3,4-b][1,4]dioxin-2-yl)methoxy)methyl)benzoic acid) (PEDOT-Ph-COOH), was electrosynthesized for the first time through the electropolymerization of the corresponding EDOT derivatives of 4-(((2,3-dihydrothieno[3,4-b][1,4]dioxin-2-yl)methoxy)methyl)-benzoic acid (EDOT-Ph-COOH). The electrochemical behavior, structural characterization, solubility, spectroscopic properties, and surface morphology of the as-prepared PEDOT-Ph-COOH films were investigated in detail. In addition, the dedoped PEDOT-Ph-COOH film got enhanced optical response, which was used as optical sensors for the determination of F^-, Cl^-, Br^-, I^-, SO_4^{2-}, HSO_4^-, NO_3^-, NO_2^-, AcO^-, SCN^-, PO_4^{3-}, CO_3^{2-}, HCO_3^-, $Cr_2O_7^{2-}$, $S_2O_3^{2-}$, K^+, Ba^{2+}, Al^{3+}, Mg^{2+}, Ca^{2+}, Sn^{2+}, Zn^{2+}, Pb^{2+}, Sr^{2+}, Cd^{2+}, Hg^{2+}, Co^{2+}, Cu^{2+}, Ni^{2+}, Pb^{2+}, Fe^{3+} Mn^{2+} on the UV absorption. It was presented that PEDOT-Ph-COOH possessed specific recognition ability for F^-, PO_4^{3-}, HCO_3^-, $S_2O_3^{2-}$, Cu^{2+}, and Fe^{3+}.

EXPERIMENTAL

Chemical Materials

4-Bromobenzoic acid ethyl ester (98%, Shanghai Baoman Biological Science and Technology Co.), sodium hydride (NaH, 60%), and potassium chloride (KCl, 99.5%), (Tianjin Damao Chemical Reagent Factory), sodium hydroxide ($\geq$99.5%), and hydrochloric acid (AR), (Shantou Xilong Chemical Industry Co.), dimethyl sulfoxide (DMSO, AR, Tianjin Bodi Chemicals Co.) were used as received; dichloromethane (CH_2Cl_2) and tetrahydrofuran (THF) were purified by distillation over calcium hydride before use; tetra-n-butylammonium hexafluorophosphate (Bu_4NPF_6, 99%; Acros Organics) was dried under vacuum at 60°C for 24 h before used; aqueous solution of K^+, Ba^{2+}, Al^{3+}, Mg^{2+}, Ca^{2+}, Sn^{2+}, Zn^{2+}, Pb^{2+}, Sr^{2+}, Cd^{2+}, Hg^{2+}, Co^{2+}, Cu^{2+}, Ni^{2+}, Pb^{2+}, Fe^{3+} Mn^{2+} were prepared from their chloride or nitrate salts, and aqueous solution of F^-, Cl^-, Br^-, I^-, SO_4^{2-}, HSO_4^-, NO_3^-, NO_2^-, AcO^-, SCN^-, PO_4^{3-}, CO_3^{2-}, HCO_3^-, $Cr_2O_7^{2-}$, $S_2O_3^{2-}$ were prepared from their potassium or sodium salts. Double-distilled deionized water used directly without further purification. Hydroxymethylated-3,4-ethylenedioxythiophene (EDOT-MeOH) was prepared according with Zhang et al.[24]

Apparatus

Electrochemical polymerization was performed in a one compartment cell using a model 263A potentiostat-galvanostat (EG&G Princeton Applied Research) under computer control. All absorption spectra were measured using an Agilent 8453 UV–Vis spectrophotometer. Fluorescence experiments were performed using a Hitachi F-4500 spectrophotometer with excitation slit set at 5 nm and emission slit at 5 nm.

The Processes of the Fabrication of Optical Sensors

A typical electrolytic solution was CH_2Cl_2-Bu_4NPF_6 (0.10 M) system containing 0.01 mol L^{-1} EDOT-Ph-COOH monomer. The amount of polymer film deposited on the surface of the electrode was controlled by the integrated current passed through the cell. To remove the electrolyte, oligomers, and monomer, polymer film was rinsed with CH_2Cl_2. As-formed PEDOT-Ph-COOH film was in the doped state and dark metal-

lic in color. For spectral analysis, polymer films were dedoped with 30% hydrochloric acid for 3 days. Films were then dried under vacuum at 60°C for 24 h. Finally, DMSO was chosen as the solvent to dissolve the dedoped PEDOT-Ph-COOH films.

Synthesis

EDOT-Ph-COOC$_2$H$_5$[37]. Under a nitrogen atmosphere, EDOT-MeOH (1.72 g, 10 mmol), KI (0.33 g, 2 mmol), and NaH (60%, 0.56 g, 14 mmol) were dissolved in THF (20 mL) with stirring while being cooled in an ice bath. A solution of 4-bromobenzoic acid ethyl ester (3.40 g, 14 mmol) in THF (20 mL) was added slowly. After the mixture was added completely, the ice bath was removed and the reaction was performed with continued stirring at 50°C overnight. After cooling to room temperature, 40 mL H_2O was added. Then the mixture was extracted with ethyl acetate (4 × 60 mL). The organic phases were combined and extracted with brine (4 × 200 mL), dried with anhydrous $MgSO_4$, and filtered. After evaporation of the solvent, the remaining crude product was isolated by flash chromatography (silica gel, petroleum ether/ethyl acetate, 9/1, v/v) to give 2.89 g of a colorless solid (yield 86%).^{1}H NMR (400 MHz, CDCl$_3$): δ 8.03 (d, $J = 8$ Hz, 2H), 7.39 (d, $J = 8$ Hz, 2H), 6.33 (t, $J = 3.6$ Hz, 2H), 4.65(s, 2H), 4.07–4.40 (m, 5H), 3.66–3.76 (m, 2H), 1.38–1.41 (m, 3H).

EDOT-Ph-COOH[38]. EDOT-Ph-COOC$_2$H$_5$ (3.25 g, 9.72 mmol) was dissolved in 20 mL THF, then added NaOH (80 mL, 20M) and stirred at 100°C overnight. The reaction mixture was allowed to cool to room temperature, 2M HCl solution was used to control the pH below 3. Subsequently, the mixture was extracted with ethyl acetate (5 × 80 mL) and the combined organic layers were washed with H_2O (3 × 200 mL), and were dried with anhydrous $MgSO_4$. After evaporation of the solvent, the remaining crude product was isolated by flash chromatography (silica gel, petroleum ether/ethyl acetate, 1/1, v/v) to give 2.78 g of a colorless oil (yield 94%).^{1}H NMR (400 MHz, CDCl$_3$): δ 8.11(d, $J = 8$ Hz, 2H), 7.45 (d, $J = 8.4$ Hz, 2H), 6.36 (s, 2H), 4.68 (t, $J = 12$ Hz, 2H), 4.39 (d, $J = 5.2$ Hz, 1H), 4.26–4.30 (m, 1H), 4.11–4.15 (m, 1H), 3.69–3.80 (m, 2H). The Efficient synthesis routes for EDOT-Ph-COOH were presented in Scheme 1.

RESULTS AND DISCUSSION

Electrochemical Polymerization of EDOT-Ph-COOH

The polymer was electrosynthesized in CH_2Cl_2-Bu_4NPF_6 (0.10 M) system containing 0.01M monomer. The representative electrochemical growth revealing the electrochemical performance of monomer and the formation of corresponding polymer are given in Figure 1. As can be seen in Figure 1, all the cyclic voltammograms (CVs) showed similar characteristics to those of other inherently conducting polymers, which indicated that the polymerization processed easily even at low monomer concentrations. In the first cycle of CVs, the current density on the reverse scan was higher than that on the forward scan [potential was in the range of −0.82–1.15 V (EDOT-Ph-COOH)]. In the Figure 1, during the oxidative scan, two oxidation peaks appeared at −0.15 and 0.33 V, and one reduction peak appeared at 48 V. All these peaks were attributed to the p-doping/dedoping processes of PEDOT-Ph-COOH film formed in
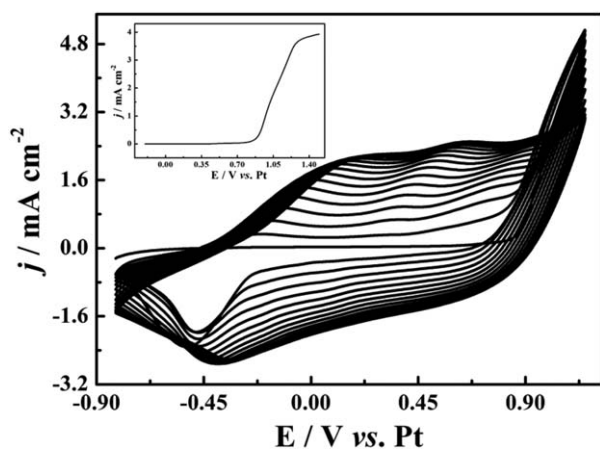
Figure 1. Cyclic voltammograms (CVs) of EDOT-Ph-COOH in CH_2Cl_2-Bu_4NPF_6 (0.1 M). Monomers concentration: 0.1 M. Potential scan rate: 100 mV s^{-1}.

previous scans. Upon sequential cycles, the redox currents increased, implying that the formation of an electroactive and conductive layer on the platinum (Pt) electrode surface (light-blue to blue-black as the deposit thickened) was gradually increasing. Moreover, the broad redox waves of the as-formed PEDOT-Ph-COOH film could be ascribed to the wide distribution of the polymer chain length or the version of conductive species on the polymer main chain from the dedoped state to polarons, from polarons to bipolarons, and finally from bipolarons to the metallic state.[39] The potential shift of the current wave maximum provided the information about the increase of the electrical resistance of the polymer films and the overpotential needed to overcome this resistance.

Potentiostatic syntheses were used to prepare PEDOT-Ph-COOH films. Considering the overall factors affecting the quality of the formed films, such as moderate polymerization rate, negligible overoxidation, regular morphology, and good adherence against the working electrode, the selected applied potential was 1.30 V for the electropolymerization of PEDOT-Ph-COOH.

Optimization of Electrical Conditions and Preparation of PEDOT-Ph-COOH

Potentiostatic electrolysis was used to prepare the newly obtained PEDOT-Ph-COOH for characterization. To optimize the applied potential for polymerization, a set of current transients during the electropolymerization of PEDOT-Ph-COOH at different applied potentials in CH_2Cl_2 were recorded, as shown in Figure 2. Typically, at applied potentials below the onset oxidation potential, no polymer film was formed on the electrode, indicating that polymerization does not occur on the electrode surface due to the low deposition voltage. Once the applied potential reaches the threshold value, all the electrosynthetic current densities experience an initial sharp increase followed by a slow decrease. The current density eventually becomes constant as a result of the uniform deposition of the polymer film on the electrode surface. At relatively high potentials, however, the surfaces of the polymer films became rough, discontinuous, and heterogeneous. Even worse, some films even fell into the solution from the electrode surface during/after the

experiments. This phenomenon was mainly due to significant overoxidation at higher potentials, which led to poor quality films. Considering the overall factors affecting the quality of the as-formed polymer film, such as moderate polymerization rate, negligible overoxidation, regular morphology, and good adherence against the working electrode, the optimized applied potential was 1.2 V vs. Pt. Therefore, PEDOT-Ph-COOH film used for the characterization mentioned below was all prepared by the chronoamperometry method at the constant potential of 1.2 V vs. Pt in CH_2Cl_2.

Infrared Spectra

Vibrational spectra can provide much structural information for conducting polymers, especially for insoluble and infusible polymers. A comparison of the evolution of the vibrational modes appearing in conducting polymers and in some simpler related molecules acting as references usually facilitates the interpretation of the experimental absorption spectra. Infrared (IR) spectra of the monomer (a), the doped (b), and dedoped (c) polymers were illustrated in Figure 3. The peak at 3111 cm^{-1} for EDOT-Ph-COOH [Figure 3(a)] was produced by C—H vibration of the 2,5-positions in the thiophene ring. This peak was retained in the monomer [Figure 3(a)] but disappeared in the electrochemical polymerized samples [Figure 3(b,c)]. This indicated that the electropolymerization of EDOT occurred at the 2,5-positions of the thiophene ring. As can be seen in Figure 3, the 3456 and 2922 cm^{-1} were closely related to the bond of COO—H of the monomer [Figure 3(a)], which were shifted to 3424 and 2922 cm^{-1} in the doped polymer [Figure 3(b)] and 3426 and 2928 cm^{-1} in the dedoped polymer [Figure 3(c)]. The strong and sharp peak at 1695 cm^{-1} was determined to be C=O of the monomer, which was shifted to 1658 and 1643 cm^{-1} in the doped and dedoped polymer, respectively. All results demonstrated that the structure of EDOT-Ph-COOH was not destroyed during the electrochemical polymerization
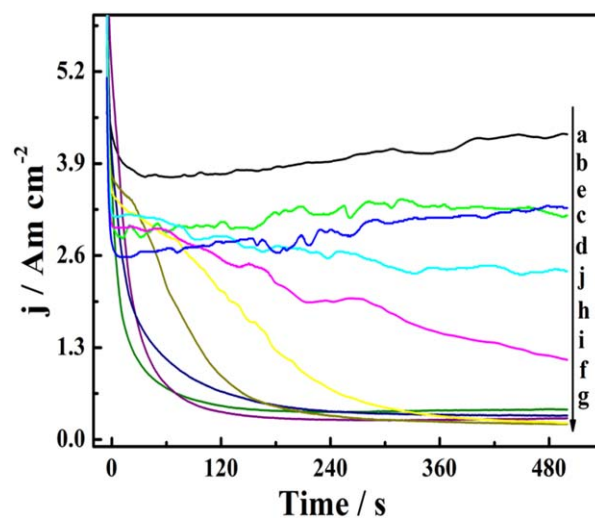

Figure 2. Chronoamperometric response of EDOT-Ph-COOH electropolymerization on three Pt electrodes for films prepared in 0.01 mol L^{-1} EDOT-Ph-COOH in CH_2Cl_2-Bu_4NPF_6 (0.1 M) by applying 1.05, 1.1, 1.15, 1.2, 1.25, 1.3, 1.35, 1.4, 1.45, and 1.5 V, respectively. [Color figure can be viewed in the online issue, which is available at wileyonlinelibrary.com.]
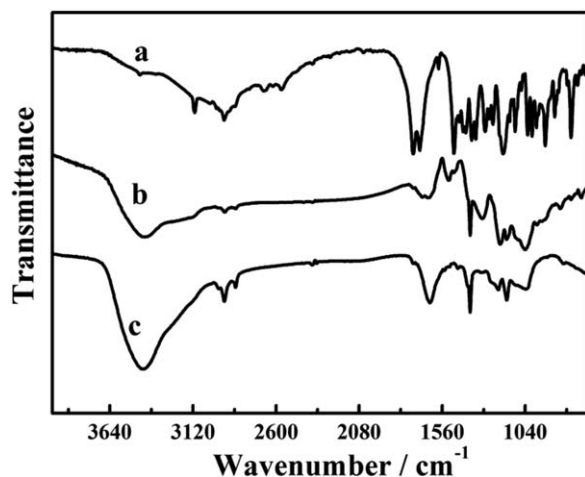
Figure 3. FT-IR spectra of monomers and polymers: EDOT-Ph-COOH (a), doped PEDOT-Ph-COOH (b), dedoped PEDOT-Ph-COOH (c).

process. Moreover, the augmented slit width and shifts of these bands from the monomer to polymer manifested the occurrence of the electrochemical polymerization.

UV–Vis and Fluorescent Spectra

PEDOT-Ph-COOH film was prepared from CH_2Cl_2-Bu_4NPF_6 in the doped state with dark brown color. When it was dedoped by 30% hydrochloric acid, its color changed to brownish yellow. It was interesting that PEDOT-Ph-COOH film was partly soluble in many common organic solvents, such as acetonitrile, DMSO, dichloromethane, tetrahydrofuran, and chloroform, etc.

UV–Vis spectra of the monomer and corresponding polymer film dissolved in DMSO were illustrated in Figure 4. The monomer of EDOT-Ph-COOH showed a characteristic absorption peak at 262 nm (a), while the spectra of the doped and dedoped PEDOT-Ph-COOH films showed two much broader absorptions with their maximum at 555 nm (b) and 564 nm (c), respectively. The overall absorption of PEDOT-Ph-COOH
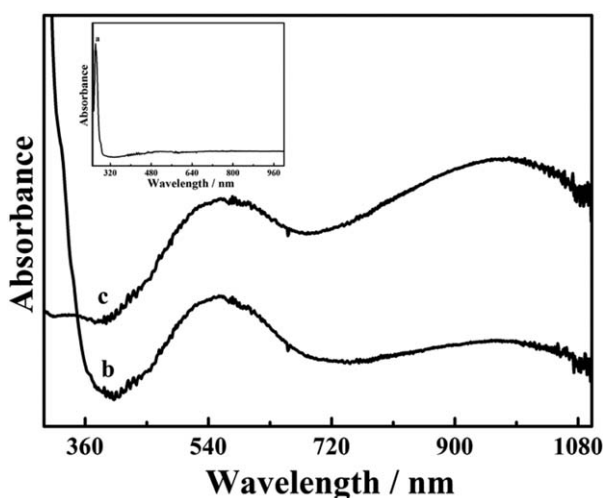
tailed off to more than 700 nm [Figure 4]. Generally, longer wavelength in spectra indicated longer polymer sequence.[40] These spectral results confirmed the occurrence of the electrochemical polymerization among the monomer and the formation of a conjugated polymer with broad molar mass distribution.

The fluorescence spectra of the monomers and corresponding polymer films in DMSO were also recorded [Figure 5]. It was observed that the emission peak of the monomer of EDOT-Ph-COOH emerged at 380 nm, whereas the dominant maximum emissions were at 611 nm for dedoped PEDOT-Ph-COOH. The obvious red shifts between the monomer and the polymer (about 230 nm) could be clearly seen from Figure 5, which were mainly attributed to the elongation of the polymers delocalized π-electron chain sequence. This further proved the formation of the conjugated backbone of PEDOT-Ph-COOH, in accordance with the UV–Vis spectral results.

Surface Morphology

Scanning Electron Microscopy (SEM) was performed to study the surface morphology of the as-prepared conducting polymer films. Microscopically, even at high magnifications, the surfaces of the doped and dedoped PEDOT-Ph-COOH films [Figure 6(a,b)] obtained from CH_2Cl_2-Bu_4NPF_6 (0.1 M) solution were rough, continuous, and homogeneous structure, which was different from the smooth surface morphology of PEDOT. The rough morphology of compact PEDOT-Ph-COOH film was extremely beneficial for the improvement of adsorption performance. In addition, there was obvious difference in surface morphology of the doped/dedoped PEDOT-Ph-COOH films. It can be clearly seen that the doped PEDOT-Ph-COOH film was columnar structure. In contrast, there was no columnar structure in the dedoped PEDOT-Ph-COOH film, and rough and compact morphology instead of the flake-like in dedoped PEDOT-Ph-COOH film. These differences between the doped and dedoped polymer films were mainly due to the migration of counteranions out of the polymer films and their gradual solubility from the electrode to the solution during the dedoping
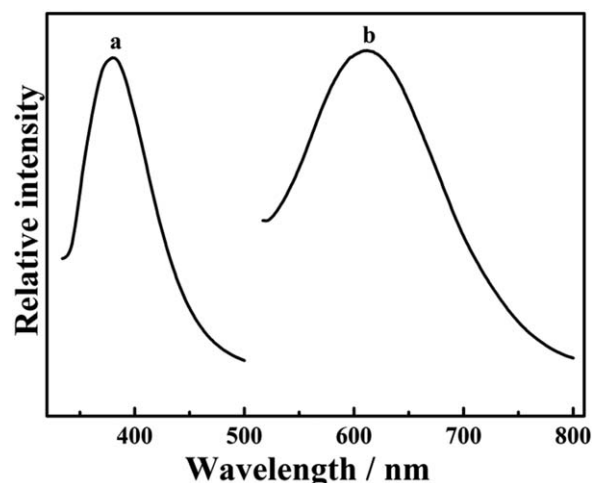

Figure 4. UV–Vis spectra of monomer and polymer: EDOT-Ph-COOH (a), doped PEDOT-Ph-COOH (b), and dedoped PEDOT-Ph-COOH (c). The monomer and polymer were dissolved in DMSO.

Figure 5. Fluorescence spectra of monomer and polymer: EDOT-Ph-COOH (a), dedoped PEDOT-Ph-COOH (b). The monomer and polymer were dissolved in DMSO.
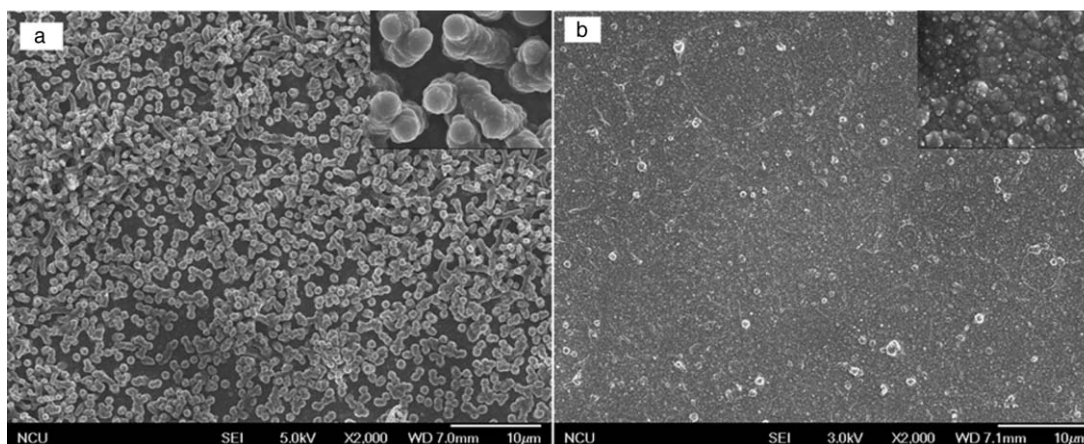
Figure 6. SEM photographs of PEDOT-Ph-COOH films deposited electrochemically on ITO electrode; doped (a) and dedoped (b) PEDOT-Ph-COOH.

processes.[41] Moreover, a rough electrode surface may give higher sensitivity than smooth surface due to increased surface area and could increase the concentration of the electroactive species. Therefore the rough and dense morphology of PEDOT-Ph-COOH film combined with different materials/molecules would improve their performance in fabricating different type sensors.[42–45]

Electrochemistry of PEDOT-Ph-COOH Film

For insight into electroactivity of the obtained polymer film, the electrochemical behavior of PEDOT-Ph-COOH film-modified electrode was investigated by cyclic voltammetry in monomer-free CH_2Cl_2-Bu_4NPF_6 (0.1 M) [Figure 7] It was clearly seen that modified electrode represented steady-state and broad redox peaks in selected electrolytes. This might be ascribed to the presence of slow diffusion of the counterions inside the film, changes of the films capacitance, and a wide distribution of the polymer chain length resulting from coupling defects distributed

statically.[46] The peak current densities were linearly proportional to the potential scanning rates [inset in Figure 7], indicating that the redox processes were nondiffusional and the electroactive polymer films were well adhered to the working electrodes surface. Furthermore, the conversion between conducting (doped) and insulating (dedoped) state was no significant decomposition, which implied the materials had high stabilities.

It is well known that the good stability of conducting polymers is significant for their applications in electronic devices.[47] Therefore, the long-term stability of the redox activity of PEDOT-Ph-COOH film was also investigated in monomer free CH_2Cl_2-Bu_4NPF_6 (0.1 M), as shown in Figure 8. The number of scanning cycles was 300 between 0.2 and 1.3 V at the potential scan rate of 150 mV s^{-1}. According to Figure 8, the polymer could be cycled repeatedly between the conducting (oxidized) and insulating (neutral) states without significant decomposition, indicating good redox stability of this material. The amount of exchange charge was remaining 74.46% after 100
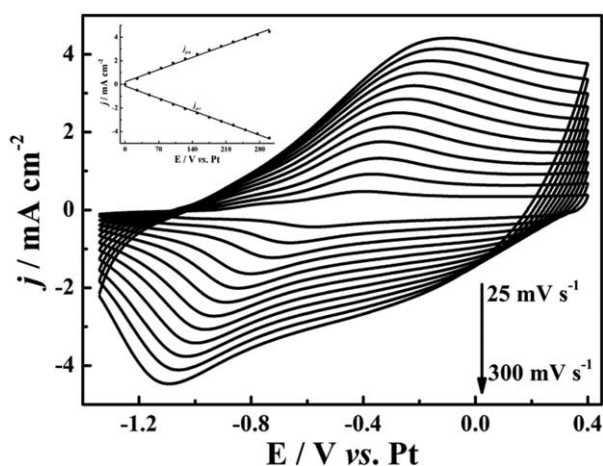

Figure 7. CVs of PEDOT-Ph-COOH film in CH_2Cl_2-Bu_4NPF_6 (0.1 M) at a potential scan rates of 25, 50, 75, 100, 125, 150, 175, 200, 225, 250, 275, and 300 mV s^{-1}. The films were obtained by CV. Inset: Plots of redox peak current densities vs. potential scan rates. j_p is the peak current densities, $j_{p.a}$ and $j_{p.c}$ denote the anodic and the cathodic peak current densities, respectively.
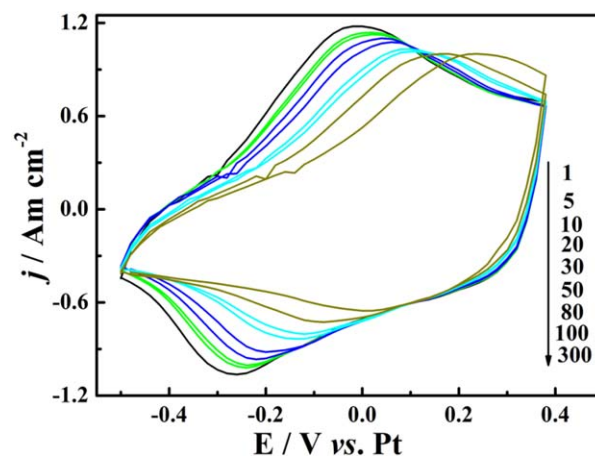

Figure 8. Successive cyclic voltammograms of PEDOT-Ph-COOH film in monomer free CH_2Cl_2-Bu_4NPF_6 (0.1 M) at the potential scan rate of 150 mV s^{-1}. [Color figure can be viewed in the online issue, which is available at wileyonlinelibrary.com.]
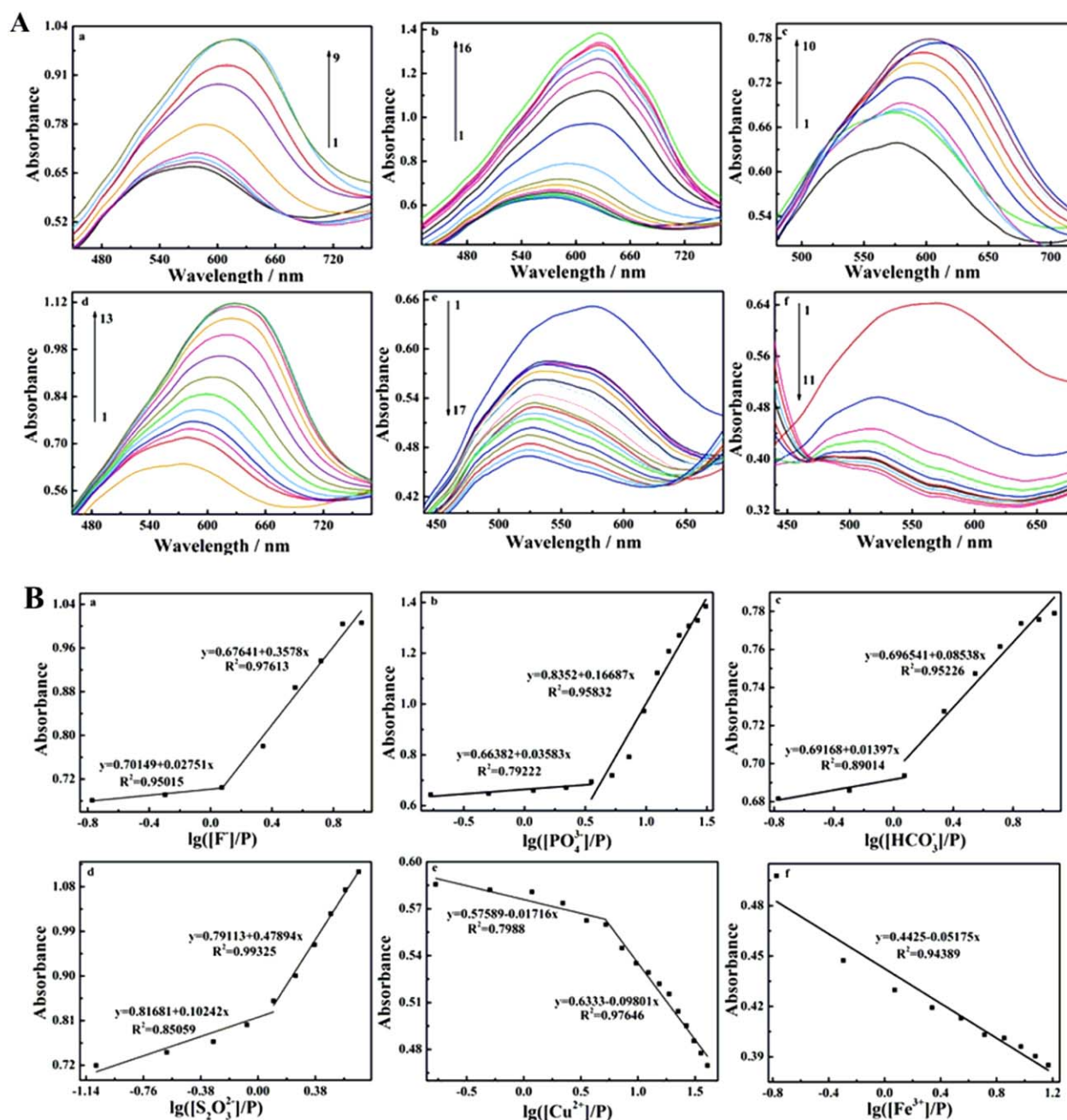
Figure 9. UV–Vis titration of PEDOT-Ph-COOH (2.69×10^{-4} M) in the DMSO with successive addition of different ions. A-(a) F^-; (b) PO_4^{3-}; (c) HCO_3^-; (d) $S_2O_3^{2-}$; (e) Cu^{2+}; (f) Fe^{3+}. B- linear range of the peak currents vs. the concentrations of F^- (a), PO_4^{3-} (b), HCO_3^- (c), $S_2O_3^{2-}$ (d), Cu^{2+} (e), and Fe^{3+} (f) ions. [Color figure can be viewed in the online issue, which is available at wileyonlinelibrary.com.]

cycles, and even after 300 cycles, PEDOT-Ph-COOH still had about 67.08% of electrochemical activity.

Application in Optical Sensors
The field of optical sensors has been a growing research area due to the advantages of non-invasive, nondestructive, continuous, and simultaneous multianalyte monitoring.[48,49] PEDOT generally showed poor photophysical properties because of its nonradiative decay via strong interchain interactions, intersystem crossing caused by heavy-atom effect of sulfur and excita-

tion annihilation between oxygen and sulfur. Therefore, some researchers studied the optical sensing application of the electropolymerization of EDOT-substituted derivatives or the copolymerization of EDOT with other units.[50,51] The PEDOT-Ph-COOH has better photophysical properties than PEDOT, because the electron-cloud density was increased on the polymer chains by introduction of saturated carbon chains, which is beneficial for the stability of excitons[52,53]; the carboxylic group as a substituent on the side chains of polymer could improve the stability of the polymer chain, and weaken the heavy-atom
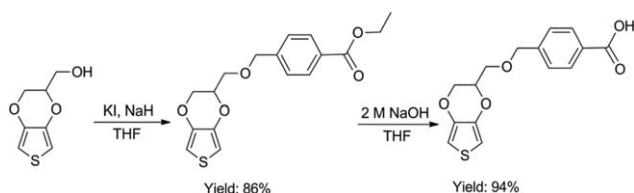
Scheme 1. Efficient synthesis routes for EDOT-Ph-COOH.[37,38]

effect of sulfur; the saturated carbon chain containing carboxylic group could change the spatial conformation of the polymer chain due to the steric hindrance. Meanwhile, this also decreased the interaction between polymer chains. In this work, optical sensors based on PEDOT-Ph-COOH were applied through UV–Vis spectroscopy.

As depicted in Figure 9(a), absorption spectra of dedoped PEDOT-Ph-COOH showed one absorption peak at 564 nm upon addition of F^- in DMSO, the values of UV absorption and the concentrations of F^- in range from 4.54×10^{-5} to 2.53×10^{-3} M [Figure 9(a)] displayed two linear relationships. The PEDOT-Ph-COOH also possessed UV absorption recognition ability for PO_4^{3-}, HCO_3^-, $S_2O_3^{2-}$, Cu^{2+}, and Fe^{3+}. The small red shift was observed by adding F^-, PO_4^{3-}, HCO_3^-, $S_2O_3^{2-}$ ions. Moreover, there were two linear ranges of the common logarithms of UV absorption intensities vs. the concentrations of PO_4^{3-} from 4.54×10^{-5} to 7.68×10^{-3} M [Figure 9(b)], HCO_3^- from 4.54×10^{-5} to 3.21×10^{-3} M [Figure 9(c)], $S_2O_3^{2-}$ from 2.27×10^{-5} to 1.74×10^{-3} M [Figure 9(d)], Cu^{2+} from 4.54×10^{-5} to 7.68×10^{-3} M [Figure 9(e)], and Fe^{3+} from 4.54×10^{-5} to 3.97×10^{-3} M [Figure 9(f)], respectively (the detail concentrations of the responding ions were put in the Supporting Information of Figure S1).

Furthermore, the selective and competitive experiments were monitored by UV spectroscopy. DMSO was used to dissolve a constant PEDOT-Ph-COOH, Figure 9(a) showed the UV quenching efficiencies of PEDOT-Ph-COOH in the presence of different ions. The effects of many inorganic ions such as F^-, Cl^-, Br^-, I^-, SO_4^{2-}, HSO_4^-, NO_3^-, NO_2^-, AcO^-, SCN^-, PO_4^{3-}, CO_3^{2-}, HCO_3^-, $Cr_2O_7^{2-}$, $S_2O_3^{2-}$, K^+, Ba^{2+}, Al^{3+}, Mg^{2+}, Ca^{2+}, Sn^{2+}, Zn^{2+}, Pb^{2+}, Sr^{2+}, Cd^{2+}, Hg^{2+}, Co^{2+}, Cu^{2+}, Ni^{2+}, Pb^{2+}, Fe^{3+} Mn^{2+} on the UV absorption of the PEDOT-Ph-COOH were investigated. Obviously, these results indicated that PEDOT-Ph-COOH possessed specific recognition ability for F^-, PO_4^{3-}, HCO_3^-, $S_2O_3^{2-}$, Cu^{2+}, and Fe^{3+}. And after added anion and/or cation solution, there was apparently color changing of host solution (the pictures were presented in the Supporting Information of Figure S2). Unfortunately, it was difficult to distinguish F^-, PO_4^{3-}, HCO_3^-, $S_2O_3^{2-}$, Cu^{2+}, and Fe^{3+} when the processes of determination were performed in the same system using the PEDOT-Ph-COOH based on UV spectroscopy. Therefore, the PEDOT-Ph-COOH structure will be further improved for distinguish detection of F^-, PO_4^{3-}, HCO_3^-, $S_2O_3^{2-}$, Cu^{2+}, and Fe^{3+}.

It is clearly observed in Figure 9 that there are red shifts in absorbance and significant spectral enhancement on addition of anions (F^-, PO_4^{3-}, HCO_3^-, $S_2O_3^{2-}$) to PEDOT-Ph-COOH. However, the addition of cations to the PEDOT-Ph-COOH is blue shifts in absorbance and significant spectral decreased.

Absorption spectra monitoring shows that there were interactions between PEDOT-Ph-COOH and ions. The red shifts in absorbance and significant spectral enhancement on addition of anions to PEDOT-Ph-COOH are due to the complexes of PEDOT-Ph-COOH with anions (F^-, PO_4^{3-}, HCO_3^-, $S_2O_3^{2-}$) through hydrogen bonding interactions are the most stable and hydrogen bonding is the primary intermolecular interactions. The carbonyl oxygen atoms of carboxylate anions of PEDOT-Ph-COOH can interact with anions (F^-, PO_4^{3-}, HCO_3^-, $S_2O_3^{2-}$) to form hydrogen bonds, which work as efficient bridges to mediate electron transfer between hydrogen-bonded species and initiate the so-called proton coupled electron transfer.[54–56] Cu^{2+} and Fe^{3+} are well-known paramagnetic ions with an empty d shell and can strongly quenching effect via electron or energy transfer.[57–59] Compared with other transition-metal ions, Cu^{2+} and Fe^{3+} have higher thermodynamic affinity and faster chelating processes toward ligands with "N" or "O" as the chelating atom.[57,60,61] Quenching of PEDOT-Ph-COOH by Cu^{2+} and Fe^{3+} is possibly due to a combination of several factors such as electron transfer, delocalization of excitons and competent energy migration along the polymer chain.

CONCLUSIONS

In this work, EDOT-Ph-COOH was synthesized by two readily synthesized steps and electropolymerized for the preparation of corresponding polymer in CH_2Cl_2-Bu_4NPF_6 (0.1 M) system. A series of characterizations were systematically tested for monomer and polymer. The obtained PEDOT-Ph-COOH film presented good redox activity, and rough surface morphology, which provided higher sensitivity than a smooth surface and increased the concentration of electroactive species combining with polymer film. More importantly, the dedoped PEDOT-Ph-COOH film possessed enhanced optical response, which was used as optical sensors for the determination of F^-, PO_4^{3-}, HCO_3^-, $S_2O_3^{2-}$, Cu^{2+}, and Fe^{3+}. The satisfactory results mentioned above also indicated that the PEDOT-Ph-COOH was an excellent sensing material. Furthermore, further research for the synthesis of EDOT derivatives based on EDOT-Ph-COOH and PEDOT-Ph-COOH as other materials, for example, thermoelectric materials and electrochromic devices, supercapacitors, fuel cells in different fields are currently ongoing and have made encouraging progress.

AUTHOR CONTRIBUTION

Substantial contribution and acquisition of all data given in this article must be given to Miss Dufen Hu. Interpretation and critical analysis of this data as a part of collaboration work between investigation groups must be given to Mr. Long Zhang and Mr. Kaixin Zhang equally. For revising the article and giving the critical opinion and also by helping to design this article, the credits must be given to Dr. Xuemin Duan and Dr. Jingkun Xu contributed as senior researchers giving the critical point note

REFERENCES

1. Groenendaal, L.; Jonas, F.; Freitag, D.; Pielartzik, H.; Reynolds, J. R. *Adv. Mater.* **2000**, *12*, 481.

2. Jonas, F.; Schrader, L. *Synth. Met.* **1991**, *41*, 831.

3. Heywang, G.; Jonas, F. *Adv. Mater.* **1992**, *4*, 116.

4. Winter, I.; Reese, C.; Hormes, J.; Heywang, G.; Jonas, F. *Chem. Phys.* **1995**, *194*, 207.

5. Dietrich, M.; Heinze, J.; Heywang, G.; Jonas, F. *J. Electroanal. Chem.* **1994**, *369*, 87.

6. Leeuw, D. M. D.; Kraakman, P. A.; Bongaerts, P. F. G.; Mutsaers, C. M. J.; Klaassen, D. B. M. *Synth. Met.* **1994**, *66*, 263.

7. Pettersson, L. A. A.; Carlsson, F.; Inganäs, O.; Arwin, H. *Thin solid Films* **1998**, *313*, 356.

8. Pei, Q. B.; Zuccarello, G.; Ahlskog, M.; Inganäs, O. *Polymer* **1994**, *35*, 1347.

9. Skotheim, T. A.; Reynolds, J. Conjugated Polymers: Processing and Application, 3rd ed.; CRC Press: Boca Raton, **2006**.

10. Skotheim, T. A.; Reynolds, J. R. Handbook of Conducting Polymers, Conjugated Polymers: Theory, Synthesis, Properties, and Characterization, 3rd ed.; CRC Press: Boca Raton, **2007**.

11. Wallace, G. G.; Spinks, G. M.; Kane-Maguire, L. A. P.; Teasdale, P. R. Conductive Electroactive Polymers: Intelligent Polymer Systems, 3rd ed.; CRC Press: Boca Raton, **2008**.

12. Groenendaal, L.; Zotti, G.; Aubert, P. -H.; Waybright, S. M.; Reynolds, J. R. *Adv. Mater.* **2003**, *15*, 855.

13. Kirchmeyer, S.; Reuter, K. *J. Mater. Chem.* **2005**, *15*, 2077.

14. Cho, S. II; Lee, S. B. *Accounts Chem. Res.* **2008**, *41*, 699.

15. Kros, A.; Nolte, R. J. M.; Sommerdijk, N. A. J. M. *Adv. Mater.* **2002**, *14*, 1779.

16. Chen, X. Y.; Yang, X. P.; Holliday, B. J. *J. Am. Chem. Soc.* **2008**, *130*, 1546.

17. Powell, A. B.; Bielawski, C. W.; Cowley, A. H. *J. Am. Chem. Soc.* **2010**, *132*, 10184.

18. Darmanin, T.; Guittard, F. *J. Am. Chem. Soc.* **2011**, *133*, 15627.

19. Wasserberg, D.; Meskers, S. C. J.; Janssen, R. A. J.; Mena-Osteritz, E.; Bäuerle, P. *J. Am. Chem. Soc.* **2006**, *128*, 17007.

20. Kim, Y. H.; Sachse, C.; Machala, M. L.; May, C.; Müller-Meskamp, L.; Leo, K. *Adv. Funct. Mater.* **2011**, *21*, 1076.

21. Liu, R.; Lee, S. B. *J. Am. Chem. Soc.* **2008**, *130*, 2942.

22. Mozer, A. J.; Panda, D. K.; Gambhir, S.; Winther-Jensen, B.; Wallace, G. G. *J. Am. Chem. Soc.* **2010**, *132*, 9543.

23. Yoon, H.; Chang, M.; Jang, J. *Adv. Funct. Mater.* **2007**, *17*, 431.

24. Zhang, L.; Wen, Y. P.; Yao, Y. Y.; Xu, J. K.; Duan, X. M.; Zhang, G. *Electrochim. Acta* **2014**, *116*, 343.

25. Gustafsson, J. C.; Liedberg, B.; Inganäs, O. *Solid State Ionics* **1994**, *69*, 145.

26. Xiao, Y. H.; Cui, X. Y.; Hancock, J. M.; Bouguettaya, M.; Reynolds, J. R.; Martin, D. C. *Sensor Actuat. B-Chem.* **2004**, *99*, 437.

27. Wen, Y. P.; Xu, J. K.; Liu, M.; Li, D.; Lu, L. M.; Yue, R. R.; He, H. H. *J. Electroanal. Chem.* **2012**, *674*, 71.

28. Havinga, E. E.; Mutsaers, C. M. J. *Chem. Mater.* **1996**, *8*, 769.

29. Kumar, A.; Welsh, D. M.; Morvant, M. C.; Piroux, F.; Abboud, K. A.; Reynolds, J. R. *Chem. Mater.* **1998**, *10*, 896.

30. Sapp, S. A.; Sotzing, G. A.; Reddinger, J. L.; Reynolds, J. R. *Adv. Mater.* **1996**, *8*, 808.

31. Han, L.; Choi, H. J.; Choi, S. J.; Liu, B. Y.; Park, D. W. *Green Chem.* **2011**, *13*, 1023.

32. Nockemann, P.; Thijs, B.; Parac-Vogt, T. N.; Hecke, K. V.; Meervelt, L. V.; Tinant, B.; Hartenbach, I.; Schleid, T.; Ngan, V. T.; Nguyen, M. T.; Binnemans, K. *Inorg. Chem.* **2008**, *47*, 9987.

33. Cheng, J. J.; Teply, B. A.; Sherifi, I.; Sung, J.; Luther, G.; Gu, F. X.; Levy-Nissenbaum, E.; Radovic-Moreno, A. F.; Langer, R.; Farokhzad, O. C. *Biomaterials* **2007**, *28*, 869.

34. Williamson, R. A.; Strange, P. G. *J. Neurochem.* **1990**, *55*, 1357.

35. Arias-Pardilla, J.; Otero, T. F.; Yu, H. H. *Electrochim. Acta* **2011**, *56*, 10238.

36. Ali, E. M.; Kantchev, E. A. B.; Yu, H.; Ying, J. Y. *Macromolecules* **2007**, *40*, 6025.

37. Luo, S. C.; Ali, E. M.; Tansil, N. C.; Yu, H.; Gao, S. J.; Kantchev, E. A. B.; Ying, J. Y. *Langmuir* **2008**, *24*, 8071.

38. Lu, B. Y.; Lu, Y.; Wen, Y. P.; Duan, X. M.; Xu, J. K.; Chen, S.; Zhang, L. *Int. J. Electrochem. Sci.* **2013**, *8*, 2826.

39. Zhou, M.; Heinze, J. *Electrochim. Acta* **1999**, *44*, 1733.

40. Bowley, H. J.; Gerrard, D. L.; Maddams, W. F.; Paton, M. R. *Macromol. Chem.* **1985**, *186*, 695.

41. Lu, B. Y.; Yan, J.; Xu, J. K.; Zhou, S. Y.; Hu, X. J. *Macromolecules* **2010**, *43*, 4599.

42. Aquino-Binag, C. N.; Kumar, N.; Lamb, R. N. *Chem. Mater.* **1996**, *8*, 2579.

43. Darain, F.; Park, D. S.; Park, J. S.; Chang, S. C.; Shim, Y. B. *Biosens. Bioelectron.* **2005**, *20*, 1780.

44. Tai, H. L.; Jiang, Y. D.; Xie, G. Z.; Yu, J. S.; Chen, X.; Ying, Z. H. *Sensor Actuat. B-Chem.* **2008**, *129*, 319.

45. Lin, K. C.; Tsai, T. H.; Chen, S. M. *Biosens. Bioelectron.* **2010**, *26*, 608.

46. Inzelt, G.; Pineri, M.; Schultze, J. W.; Vorotyntsev, M. A. *Electrochim. Acta* **2000**, *45*, 2403.

47. Uckert, F.; Tak, Y. -H.; Müllen, K.; Bässler, H. *Adv. Mater.* **2000**, *12*, 905.

48. Ulber, R.; Frerichs, J. G.; Beutel, S. *Anal. Bioanal. Chem.* **2003**, *376*, 342.

49. McDonagh, C.; Burke, C. S.; MacCraith, B. D. *Chem. Rev.* **2008**, *108*, 400.

50. Anzenbacher, P.; Jursikova, K.; Aldakov, D.; Marquez, M.; Pohl, R. *Tetrahedron* **2004**, *60*, 11163.

51. Zhang, K.; Tieke, B.; Forgie, J. C.; Skabara, P. J. *Macromol. Rapid Comm.* **2009**, *30*, 1834.

52. Fahlman, M.; Salaneck, W. R. *Surf. Sci.* **2002**, *500*, 904.

53. Kulkarni, A. P.; Jenekhe, S. A. *Macromolecules* **2003**, *36*, 5285.

54. Lee, S. K.; Kim, H.; Jang, S.; Kang, J. *Tetrahedron Lett.* **2011**, *52*, 1977.

55. Zhang, X.; Guo, L.; Wu, F. Y.; Jiang, Y. B. *Org. Lett.* **2003**, *5*, 2667.

56. Zhang, G.; Wen, Y. P.; Li, Y. Z.; Xu, J. K.; Guo, C. Q.; Lu, B. Y.; Zhu, D. H. *J. Fluoresc.* **2013**, *23*, 1053.

57. Krämer, R. *Angew. Chem. Int. Edit.* **1998**, *37*, 772.

58. Zhang, X. B.; Cheng, G.; Zhang, W. J.; Shen, G. L.; Yu, R. Q. *Talanta* **2007**, *71* 171.

59. Lohani, C. R.; Lee, K. -H. *Sensor Actuat. B-Chem.* **2010**, *143*, 649.

60. De Silva, A. P. H.; Gunaratne, Q. N.; Gunnlaugsson, T.; Huxley, A. J. M.; McCoy, C. P.; Rademacher, J. T.; Rice, T. E. *Chem. Rev.* **1997**, *97*, 1515.

61. Zhang, G.; Lu, B. Y.; Wen, Y. P.; Lu, L. M.; Xu, J. K. *Sensor Actuat. B-Chem.* **2012**, *171*, 786.